Immune Network
http://dx.doi.org/10.4110/in.2013.13.3.94
pISSN 1598-2629 eISSN 2092-6685
ORIGINAL ARTICLE

Immunostimulatory Effects of Silica Nanoparticles in Human Monocytes

*Eun-Jeoung Yang and In-Hong Choi**

Department of Microbiology, The Institute for Immunology and Immunological Diseases, Yonsei University College of Medicine, Seoul 120-752, Korea

Amorphous silica particles, whose applications are increasing in many biomedical fields, are known to be less toxic than crystalline silica. In this study, the inflammatory effects of amorphous silica nanoparticles were investigated using 30-nm amorphous silica nanoparticles and human peripheral blood mononuclear cells (PBMCs) or purified monocytes. As a result, production of IL-1β and IL-8 were increased. In addition, the mitochondrial reactive oxygen species (ROS) was detected, which may lead to mitochondrial membrane disruption. Most importantly, inflammasome formation was observed. Therefore, these results provide immunological information about amorphous silica nanoparticles and suggest that amorphous silica nanoparticles can evoke innate immune reactions in human monocytes through production of IL-1β and IL-8.

[Immune Network 2013;13(3):94-101]

INTRODUCTION

Silica nanoparticles have been used in various fields, such as chemical mechanical engineering, drug delivery, cosmetics, printer tones, varnishes, and additives for foods (1-5). Recently, the applications have been widened to biomedical and biotechnological areas, including biosensors for simultaneous assay of glucose, lactate, L-glutamate, and hypoxanthine levels in rat striatum (6), biomarkers for leukemia cell identification using optical microscopic imaging (7), cancer therapy (1), DNA delivery (2,8), and drug delivery (9).

As commodities containing silica nanoparticles have been increasing, chances of exposure to silica nanoparticles have also been increasing. To date, research into toxicity of silica particles has focused on 0.5− to 10-μm crystalline silica. However, nano-sized (smaller than 100 nm) silica particles, which are becoming more popular these days, apparently possess unique toxicological properties compared to 0.5− to 10-μm silica particles (10). Among crystalline and amorphous forms of silica (silicon dioxide, SiO_2), the commonest forms of free crystalline silica include quartz, tridymite, and cristobalite. Natural quartz exists in sandstone (67% silica) and granite (25～40% silica). Amorphous silica can be found in diatomaceous earth, opal, silica, and glass (11).

Inhalation of small silica crystals causes acute pulmonary inflammation. Chronic occupational exposure to silica crystals may induce pneumoconiosis silicosis, which results in progressive lung fibrosis. However, underlying mechanisms for pulmonary inflammation and fibrosis have not yet been fully identified (12). After inhaled silica crystals are deposited in small airways and phagocytized by resident macrophages, pulmonary alveolar macrophages secrete IL-1β or TNF (tumor necrosis factor)-α to induce inflammation and TGF (transforming growth factor)-β to induce fibrosis. During the process, apoptotic cell death occurs to remove unhealthy cells containing silica particles. Then, silica particles released from dying cells are phagocytized by neighboring macrophages,

Received on May 9, 2013. Revised on May 22, 2013. Accepted on May 30, 2013.

*Corresponding Author. In-Hong Choi, Department of Microbiology, Yonsei University College of Medicine, Seoul, Korea. Tel: 82-2-2228-1821; Fax: 82-2-392-7088; E-mail: inhong@yuhs.ac

Keywords: Silica nanoparticles, Human monocytes, Cytokine, Inflammasome, Mitochondrial membrane

Abbreviations: ROS, reactive oxygen species; PBMC, peripheral blood monocyte; IL, interleukin

which evokes further inflammation (13).

Amorphous silica particles are known to be less toxic than crystalline silica. However, the applications of amorphous silica have been increasing, and nano-sized amorphous silica particles have become popular in many biomedical fields. Therefore, we investigated the inflammatory effects of amorphous silica nanoparticles using 30-nm amorphous silica nanoparticles and assessed their effects on human peripheral blood mononuclear cells (PBMCs) or purified monocytes. Cytotoxicity and production of IL-1β and IL-8 were evaluated. The mitochondrial ROS, mitochondrial membrane integrity, inflammasome formation, and endosomal localization of silica nanoparticles were also assessed.

MATERIALS AND METHODS

Cell culture and cell purification

After internal review board approval and informed consent (No: 4-2012-0088), 100-ml blood was obtained from ten healthy donors. PBMCs were separated using ficoll/hypaque density gradient (density=1.070−1.074) by centrifugation at 1,600 rpm for 25 min. PBMCs were cultured in RPMI 1640 containing 10% FBS and streptomycin/penicillin (each 100 IU/mL) at 37°C in a moisturized 5% CO_2 incubator. Although endotoxin was not detected in silica nanoparticles used in this study, polymyxin B (InvivoGen, San Diego, CA, USA) at a concentration of 10 ng/ml was added as an endotoxin neutralizer. To purify monocytes, PBMCs were incubated for 2 h in RPMI 1640 containing 1% FBS at 37°C in a moisturized 5% CO_2 incubator, and adherent cells were obtained after discarding non-adherent cells. Staining for CD14, a monocyte marker, was performed to identify the monocyte population.

Cytotoxicity assay

Cell was assessed using a colorimetric cell counting kit-8 (CCK-8) (Dojindo laboratories, Kyoto, Japan). CCK-8 is based on a colorimetric assay utilizing a highly water soluble tetrazolium salt, WST-8 [2-(2-methyxy-4-nitrophenyl)-3-(4-nitrophenyl)-5-(2,4-disulfophenyl)-^{2}H-tetrazolium, monosodium salt]. Wells were treated with 200 μl of silica nanoparticle solutions diluted in cell culture medium. After 6 h, 15 μl of CCK-8 reagent was added to each well and then incubated at 37°C for 2 h. After centrifugation, 100 μl of the supernatant was transferred to 96-well microtiter plates, and optical densities (OD) were measured at 450 nm with a spectrophotometer (Molecular Devices, Sunnyvale, CA, USA) to avoid optical interference caused by silica nanoparticles. LPS (*E. coli* 026:B6; Sigma-Aldrich, St Louis, MO, USA) was treated at 25 ng/ml for 1 h before exposure of PBMCs to nanoparticles.

Enzyme-linked immunosorbent assay (ELISA)

ELISA was performed to assess IL-1β and IL-8 in the culture supernatant. PBMCs were plated in 24-well plates at 2×10^5 cells per well in 200 μl of RPMI 1640 containing 10% FBS. Silica nanoparticles in cell culture media were added to each well, making the final volume of 400 μl per well. After culture times were recorded, cell culture supernatants were collected and stored at −80°C. ELISA was performed with a human IL-1β and IL-8 assay kits (BD Biosciences, San Jose, CA, USA) which use biotinylated anti-IL-1β and anti-IL-8, detection antibodies, and streptavidin-horse radish peroxidase. OD values were read at 450 nm.

Staining with MitoSOX and JC-1

Monocytes were treated with silica nanoparticles (125 and 250 μg/ml for 30-nm silica particles) for 40 min for MitoSOX staining (for 15 min). After treatment with silica nanoparticles, blood monocytes were stained with fluorescent dyes (MitoSOX) diluted in Hank·s balanced salt solution for 15∼30 min at 37°C in the dark. Then, 2.5 μM MitoSOX (Invitrogen, San Diego, CA, USA) was applied to detect mitochondrial superoxide. After exposure to silica nanoparticles, staining with 2 μM JC-1 (Invitrogen) was performed to determine mitochondrial depolarization. Flow cytometric analysis was performed using a FACScan (Becton Dickinson, Franklin Lakes, NJ, USA), and the results were analyzed using WinMDI software.

TEM analysis

Monocytes were treated with 125 μ/ml of silica nanoparticles for 15 min and fixed with Karnovsky solution (2% glutaraldehyde, 2% paraformaldehyde, 0.5% $CaCl_2$) for 6 h. After washing with PBS for 2 h, cells were treated with 1% OsO_4 in 0.1M PBS for 2 h. Dehydration of each sample was performed gradually with 50%, 60%, 70%, 80%, 90%, 95% and 100% alcohol for 10 min, followed by a final addition of propylene oxide for 10 min. Samples were then treated with a mixture of EPON (EPON 812, MNA, DDSA, DMP30) and propylene oxide (1 : 1) for 18 h and heated in an embedding oven at 35°C for 6 h, 45°C for 12 h, and 60°C for 24 h. The cell block was trimmed and sectioned at 0.25 μm using an ultramicrotome (Leica Ultracut UCT, Leica Microsystems

GmbH, Wetzlar, Germany). These ultra-thin sections were stained with 1% toluidine blue and put on a copper grid. The samples were then stained with both uranyl acetate (6%) and lead citrate, and analyzed using a TEM (JEM-1011, JEOL, Tokyo, Japan).

Statistical analysis

Independent Student's t test and one-way analysis of variance (ANOVA) were used to compare the differences between the control and study groups. A p-value of <0.05 was considered significant.

RESULTS

Cytotoxicity and cytokine production by PBMCs after exposure to 30 nm amorphous silica nanoparticles

The cytotoxicity of 30-nm silica nanoparticles in PBMCs has increased dose-dependently (Fig. 1a) starting at a concentration of 31.3 μ/ml. Similar results were obtained after pretreatment with a low concentration (25 ng/ml) of LPS for 3 h (Fig.

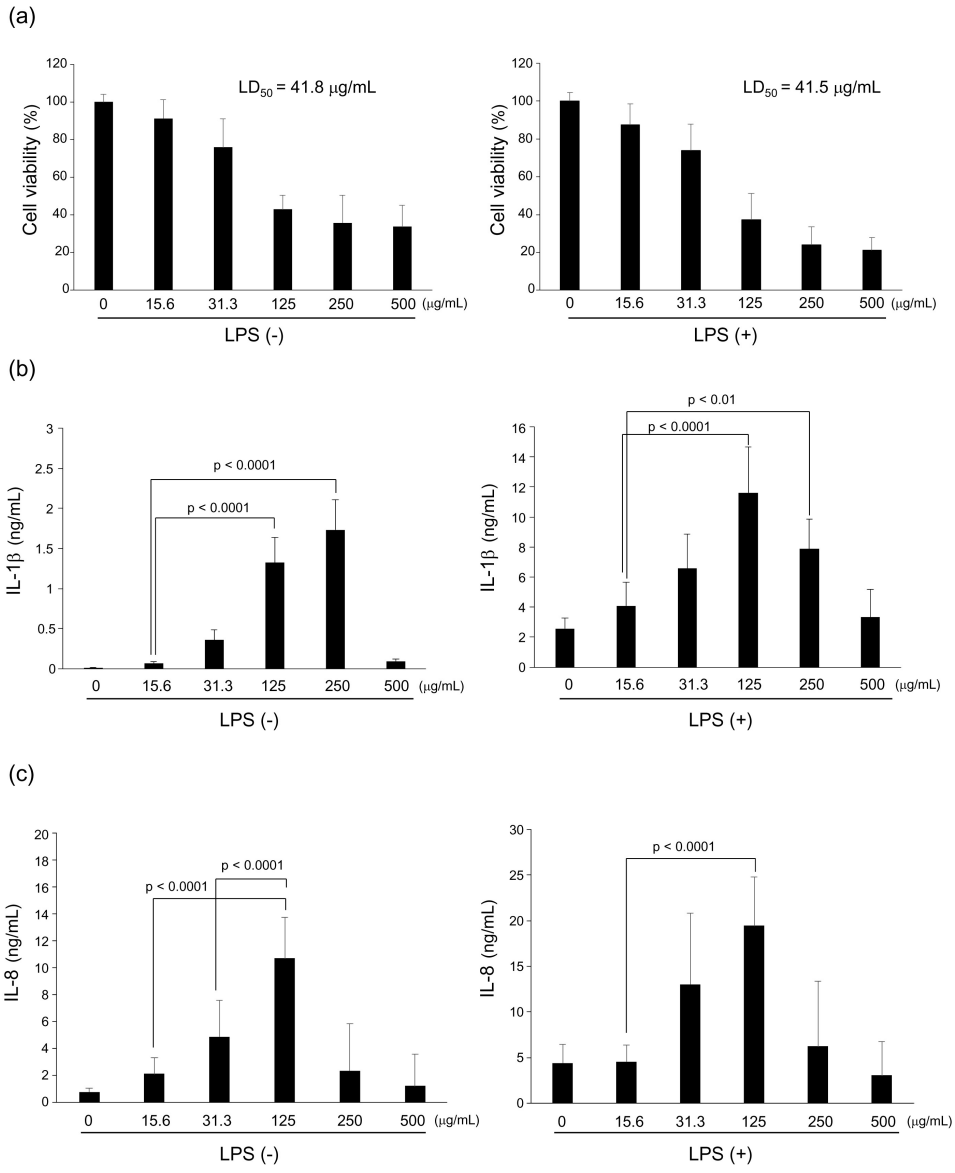

Figure 1. Cytotoxicity and production of cytokines in PBMCs. (a) PBMCs were treated with 30-nm amorphous silica nanoparticles for 6 h and cytotoxicity was determined by CCK-8 assay. (b, c) PBMCs were treated with silica nanoparticles for 6 h and supernatant levels of IL-1β (b) and IL-8 (c) were assessed by ELISA. LPS (25 ng/ml) was pretreated for 3 h before nanoparticle exposure. Data represent means$\pm$ S.D. of three independent experiments. One-way ANOVA analysis shows significance ($p<0.0001$) (b, c) and student's t-test between certain pairs (b, c) was used for statistical analysis.

1a). The LD_{50} values of silica nanoparticles were 41.8 μg/ml without LPS and 41.4 μg/ml with LPS. Therefore, the pretreatment with LPS at a low concentration did not influence cytotoxicity following exposure to silica nanoparticles.

After exposure to silica nanoparticles, the levels of IL-1β and IL-8 produced by PBMCs increased dose-dependently. The IL-1β levels were 0.4, 1.3, and 1.7 ng/ml after treatment with silica nanoparticle at concentrations of 31.3, 125, and 250 μg/ml, respectively. When LPS was pretreated, the IL-1β levels were higher (6.6, 11.6, and 7.9 ng/ml after treatment with silica nanoparticles at concentrations of 31.3, 125, 250 μg/ml, respectively) than those treated with silica nanoparticles alone (Fig. 1b). The IL-8 levels were 4.9, 10.7, and 2.4 ng/ml after treatment with silica nanoparticles at concentrations of 31.3, 125, and 250 μg/ml, respectively. When LPS was pretreated, the IL-8 levels were higher (13.1, 19.4, and 6.3 ng/ml after treatment with silica nanoparticles at concentrations of 31.3, 125, and 250 μg/ml) than those treated with silica nanoparticles alone (Fig. 1c). After pretreatment with LPS, production of IL-8 started to decrease at a silica nanoparticle concentration of 250 μg/ml. After pretreatment with LPS, production of IL-1β or IL-8 started to decrease at a silica nanoparticle concentration of 250 μg/ml. These results suggest that PBMCs primed with LPS become vulnerable to the following stimuli. Therefore, PBMCs respond more sensitively at lower concentrations of the following stimuli, but they become exhausted and do not respond to higher concentrations of the following stimuli.

Superoxide generation and deterioration of mitochondrial membranes in monocytes

After purification of monocytes from PBMCs, generation of superoxide was detected by MitoSOX and expressed as MI. As shown in Fig. 2, the MIs were 497 at a silica nanoparticle concentration of 125 μg/ml and 555 at a silica nanoparticle concentration of 250 μg/ml. When compared to the results of 5-nm silver nanoparticles, which were used as a positive control, silica nanoparticles induced significantly lower levels of superoxide. Silica nanoparticles operated at higher concentrations than silver nanoparticles, which was due to different characteristics of individual nanoparticles. The LD_{50} of 5-nm silver nanoparticles is 0.48 μg/ml (14), whereas that of 30 nm silica particles is 41.8 μg/ml. In our study, 100-nm silver nanoparticles were used as a negative control because they do not trigger monocytes at 0.6~0.9 μg/ml (14).

Since MitoSOX detects superoxide at mitochondrial membrane, which may induce deterioration of mitochondrial membrane, we assessed mitochondrial membrane potential.

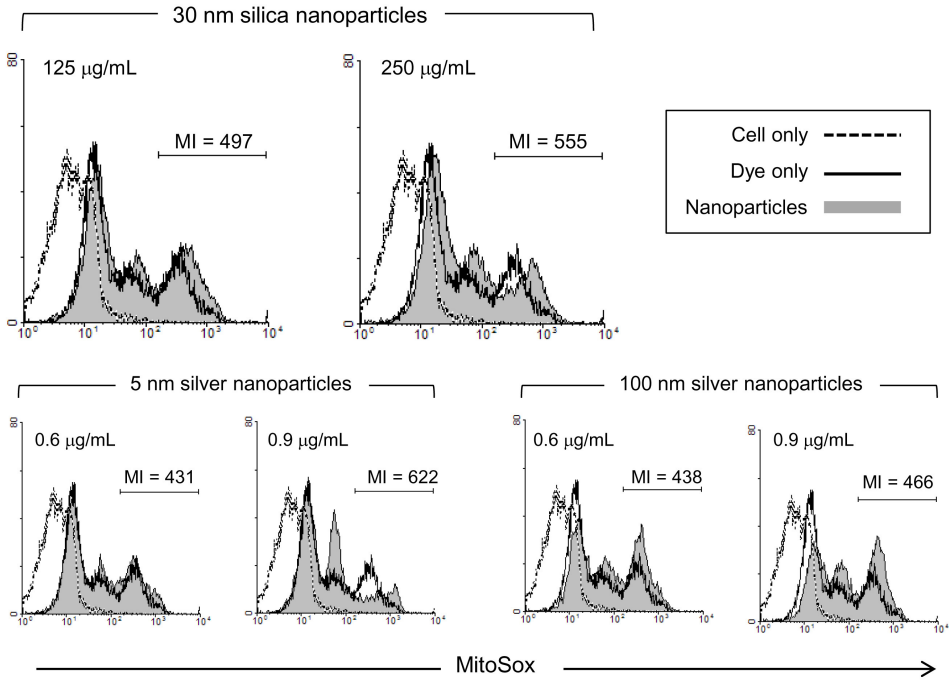

Figure 2. Production of mitochondria ROS in blood monocytes. Monocytes were treated with silica nanoparticles or silver nanoparticles for 40 min. Cells were stained with 2.5 μM MitoSOX (for mitochondrial superoxide) for 15 min and analyzed by flow cytometry. MI, mean intensity. Data shown here are representative results from three independent experiments.

JC-1 staining revealed the disturbance of mitochondrial membrane after exposure to 30-nm silica nanoparticles. The percentage of mitochondrial staining decreased by 51.5% at 1 h, by 50.4% at 1.5 h, and by 50.0 % at 2 h (Fig. 3). The control level was 60.5%, which was detected without exposure to silica nanoparticles.

Inflammasome formation in monocytes

To determine the inflammasome formation by silica nanoparticles, monocytes were stained with anti-NLRP3 and anti-caspase-1 antibodies after exposure to nanoparticles. As a result, oligomerization of NLRP3 and caspase-1 was detected 15 min after exposure to silica nanoparticles at a concentration of 125 μg/ml (Fig. 4). Oligomerization of NLRP3 and caspase-1 was not found in control cells which were not exposed to silica nanoparticles.

Endocytosis of silica nanoparticles in monocytes

Next, the presence of silica nanoparticles and intracellular changes in monocytes were assessed via TEM. Within 30 min after treatment with silica nanoparticles at a concentration of 125 μg/ml, double membrane structures suggestive of autophagosomes were found as indicated with white arrows (Fig. 5a). Silica nanoparticles also were detected in endosomes (Fig. 5b).

DISCUSSION

The aim of this study was to provide information on inflammatory effects of amorphous silica nanoparticles. As reported previously, crystalline silica nanoparticles induce NLRP3 inflammasome to secrete IL-1β, which is mediated by particle uptake, rupture of lysosomal membrane, and release of cathepsin B (15,16). The subsequent secretion of IL-1β is known to be responsible for silicosis (17). In contrast, the results from amorphous silica nanoparticles vary depending on particle size and cell types (18-20). Therefore, in our study using human PBMCs or purified monocytes, the effects of amorphous silica nanoparticles were assessed.

Maturation of IL-1β is tightly regulated by NLRP3, 1 of the 4 inflammasome types (21). Thus, even if pro-IL-1β protein is present inside a cell, it cannot be released until NLRP3 inflammasomes are formed. Upon proper assembly of NLRP3 inflammasomes, caspase-1 is activated and cleaves the pro-form of IL-1β to generate mature IL-1β. Mature IL-1β is then released from cells to perform their respective immunological

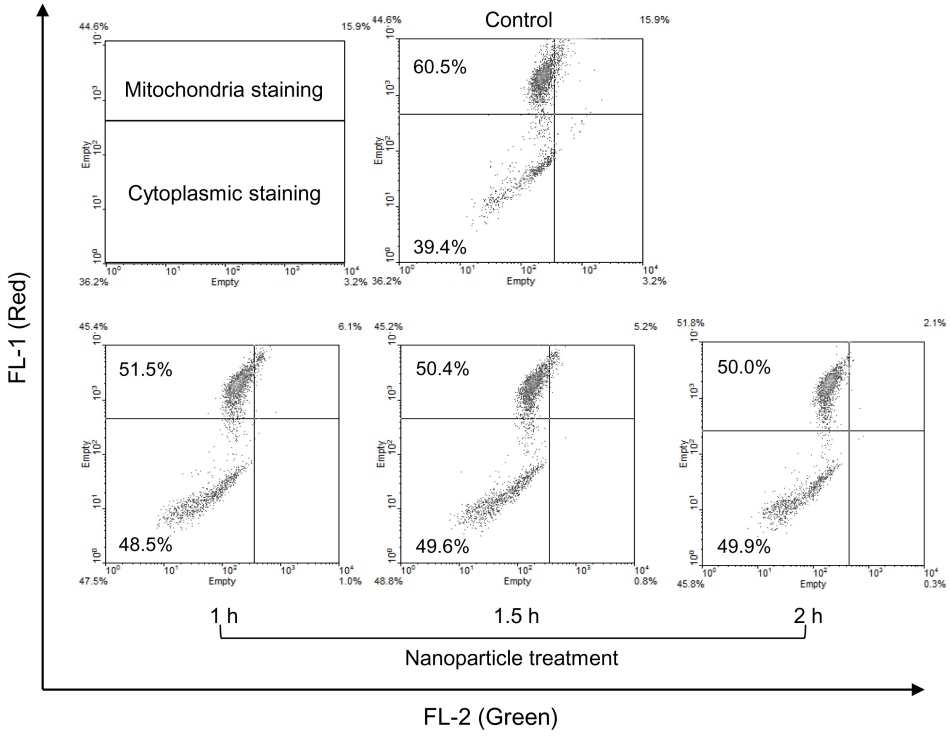

Figure 3. Assessment of mitochondrial membrane integrity. Monocytes were treated with 125 μg/ml of 30 nm silica nanoparticles for 1 h, 1.5 h, and 2 h. After exposure for the indicated time, JC-1 (2 μM) staining was performed to evaluate disturbance of mitochondrial membranes. Cells stained as red (intact mitochondria) were determined by flow cytometry. Data shown here are representative results from three independent experiments. MI, mean intensity.

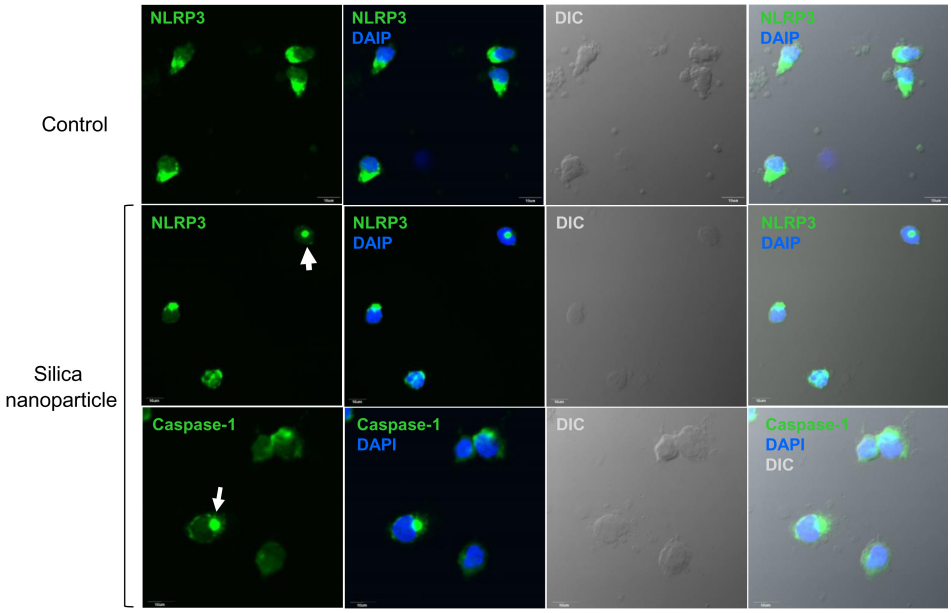

Figure 4. Inflammasome formation of caspase-1 and NLRP3 in monocytes. To analyze oligomerization of NLRP3 and caspase-1, monocytes were treated with silica nanoparticles (125 μg/ml) for 15 min. Oligomerization of NLRP3 and caspase-1 was assessed by confocal microscopy after staining with anti-NLRP3 and anti-caspase-1 antibodies. White arrows indicate oligomerization of each molecule, which are not observed in controls.

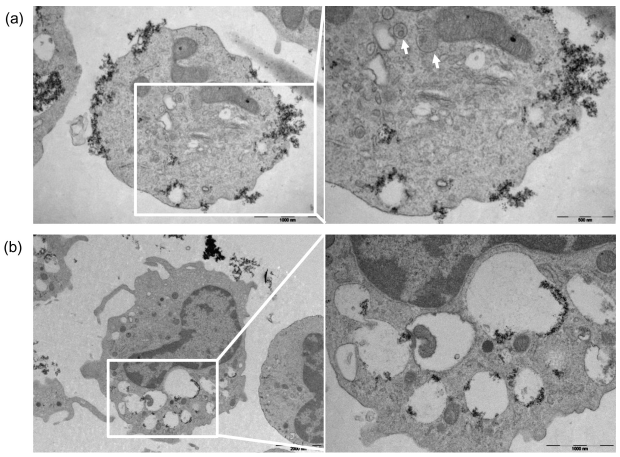

Figure 5. TEM images of monocytes after exposure to silica nanoparticles. Monocytes were treated with silica nanoparticles (125 μg/ml) for 30 min. After 30 nm silica nanoparticle exposure, (a) double membrane structures (white arrows) suggesting autophagy-like structures and (b) presence of silica nanoparticles were observed inside endosome.

functions. Therefore, factors triggering inflammasome formation are also critical for producing functional IL-1β.

We assessed the responses of human PBMCs after treatment with silica nanoparticles. As expected, 30-nm amorphous silica nanoparticles induced IL-1β production in human PBMCs. We further speculated that silica nanoparticles may increase IL-1β production when pretreated with a low concentration of LPS. These findings suggest that the immunological relevance of silica nanoparticles should be considered with regard to their synergistic effects on minimally activated immune responses.

To simulate an *in vivo* environment we purified monocytes from PBMCs and assessed inflammasome formation. Previous immunological studies with nanoparticles mainly focused on macrophage cell lines, but not primary monocytes. It has been reported that macrophages and monocytes have different pathways to produce inflammasomes. While macrophages require 2 signals to release mature IL-1b, the first signal to produce pro-IL-1β protein and the second signal to activate NLRP3, monocytes constitutively express active caspse-1 and require only 1 signal for IL-1β release (22).

To activate caspase-1, inflammasome formation is a prerequisite. During inflammasome formation, oligomerization of NLRP3 occurs simultaneously with oligomerization of caspase-1. Confocal findings of monocytes treated with 30-nm silica nanoparticles suggest that oligomerization of NLRP3 or caspase-1 occurs rapidly as early as 15 min after exposure to nanoparticles. We investigated mechanisms underlying inflammasome formation following exposure to silica nanoparticles. ROS has been suggested to be a causative factor in the induction of the inflammasome complex. There have been many reports on the sources of ROS, such as peroxisomes, nitric oxide synthases, oxidoreductin 1, and cytosolic enzymes including cyclooxygenase, in the endoplasmic retic-

ulum (23,24). However, the majority of ROS are produced as a by-product of the mitochondrial electron transport chain in cells undergoing aerobic metabolism (25). Although TiO_2 (26), silica (27) and silver nanoparticles (14) produce ROS, there have been few reports that have identified the types of ROS produced. In our study, ROS was evaluated by assessing the production of mitochondria superoxide. Recently, superoxide in the mitochondrial membrane was reported to trigger inflammasome formation (14,28) in specific structures called mitochondria-associated ER membranes (29). Our results showed that 30-nm silica nanoparticles more increased production of mitochondrial superoxide than 100-nm silver nanopaticles and that collapse of the mitochondrial membrane was observed in blood monocytes 1 h, 1.5 h, and 2 h after treatment with 30-nm silica nanoparticles.

Collectively, inflammasome formation in monocytes was observed after exposure to amorphous silica nanoparticles. However, rupture of the endolysosomal membrane which was shown in crystalline silica was not detected in our study. These findings suggest that induction of superoxide and subsequent deterioration of the mitochondrial membrane may be one of the major factors in the induction of inflammasome formation in amorphous silica nanoparticles.

ACKNOWLEDGEMENTS

This research was supported by a National Research Foundation of Korea Grant funded by the Korean Government (MIST) (NRF-2009-0082417).

CONFLICTS OF INTEREST

The authors have no financial conflict of interest.

REFERENCES

1. Hirsch, L. R., R. J. Stafford, J. A. Bankson, S. R. Sershen, B. Rivera, R. E. Price, J. D. Hazle, N. J. Halas, and J. L. West. 2003. Nanoshell-mediated near-infrared thermal therapy of tumors under magnetic resonance guidance. *Proc. Natl. Acad. Sci. U. S. A.* 100: 13549-13554.
2. Bharali, D. J., I. Klejbor, E. K. Stachowiak, P. Dutta, I. Roy, N. Kaur, E. J. Bergey, P. N. Prasad, and M. K. Stachowiak. 2005. Organically modified silica nanoparticles: a nonviral vector for in vivo gene delivery and expression in the brain. *Proc. Natl. Acad. Sci. U. S. A.* 102: 11539-11544.
3. Roy, I., T. Y. Ohulchanskyy, D. J. Bharali, H. E. Pudavar, R. A. Mistretta, N. Kaur, and P. N. Prasad. 2005. Optical tracking of organically modified silica nanoparticles as DNA carriers: a nonviral, nanomedicine approach for gene delivery. *Proc. Natl. Acad. Sci. U. S. A.* 102: 279-284.
4. Bottini, M., F. D'Annibale, A. Magrini, F. Cerignoli, Y. Arimura, M. I. Dawson, E. Bergamaschi, N. Rosato, A. Bergamaschi, and T. Mustelin. 2007. Quantum dot-doped silica nanoparticles as probes for targeting of T-lymphocytes. *Int. J. Nanomedicine* 2: 227-233.
5. Verraedt, E., M. Pendela, E. Adams, J. Hoogmartens, and J. A. Martens. 2010. Controlled release of chlorhexidine from amorphous microporous silica. *J. Control. Release.* 142: 47-52.
6. Zhang, F. F., Q. Wan, C. X. Li, X. L. Wang, Z. Q. Zhu, Y. Z. Xian, L. T. Jin, and K. Yamamoto. 2004. Simultaneous assay of glucose, lactate, L-glutamate and hypoxanthine levels in a rat striatum using enzyme electrodes based on neutral red-doped silica nanoparticles. *Anal. Bioanal. Chem.* 380: 637-642.
7. Santra, S., P. Zhang, K. Wang, R. Tapec, and W. Tan. 2001. Conjugation of biomolecules with luminophore-doped silica nanoparticles for photostable biomarkers. *Anal. Chem.* 73: 4988-4993.
8. Gemeinhart, R. A., D. Luo, and W. M. Saltzman. 2005. Cellular fate of a modular DNA delivery system mediated by silica nanoparticles. *Biotechnol. Prog.* 21: 532-537.
9. Slowing, I. I., J. L. Vivero-Escoto, C. W. Wu, and V. S. Lin. 2008. Mesoporous silica nanoparticles as controlled release drug delivery and gene transfection carriers. *Adv. Drug Deliv. Rev.* 60: 1278-1288.
10. Maynard, A. D., R. J. Aitken, T. Butz, V. Colvin, K. Donaldson, G. Oberdörster, M. A. Philbert, J. Ryan, A. Seaton, V. Stone, S. S. Tinkle, L. Tran, N. J. Walker, and C. B. Warheit. 2006. Safe handling of nanotechnology. *Nature* 444: 267-269.
11. Greenberg, M. I., J. Waksman, and J. Curtis. 2007. Silicosis: a review. *Dis. Mon.* 53: 394-416.
12. Mossman, B. T. and A. Churg. 1998. Mechanisms in the pathogenesis of asbestosis and silicosis. *Am. J. Respir. Crit. Care. Med.* 157: 1666-1680.
13. Huaux, F. 2007. New developments in the understanding of immunology in silicosis. *Curr. Opin. Allergy. Clin. Immunol.* 7: 168-173.
14. Yang, E. J., S. Kim, J. S. Kim, and I. H. Choi. 2012. Inflammasome formation and IL-1β release by human blood monocytes in response to silver nanoparticles. *Biomaterials* 33: 6858-6867.
15. Hornung, V., F. Bauernfeind, A. Halle, E. O. Samstad, H. Kono, K. L. Rock, K. A. Fitzgerald, and E. Latz. 2008. Silica crystals and aluminum salts activate the NALP3 inflammasome through phagosomal destabilization. *Nat. Immunol.* 9: 847-856.
16. Dostert, C., V. Pétrilli, R. Van Bruggen, C. Steele, B. T. Mossman, and J. Tschopp. 2008. Innate immune activation through Nalp3 inflammasome sensing of asbestos and silica. *Science* 320: 674-677.
17. Cassel, S. L., S. C. Eisenbarth, S. S. Iyer, J. J. Sadler, O. R. Colegio, L. A. Tephly, A. B. Carter, P. B. Rothman, R. A. Flavell, and F. S. Sutterwala. 2008. The Nalp3 inflammasome

is essential for the development of silicosis. *Proc. Natl. Acad. Sci. U. S. A.* 105: 9035-9040.
18. Morishige, T., Y. Yoshioka, H. Inakura, A. Tanabe, X. Yao, S. Narimatsu, Y. Monobe, T. Imazawa, S. Tsunoda, Y. Tsutsumi, Y. Mukai, N. Okada, and S. Nakagawa. 2010. The effect of surface modification of amorphous silica particles on NLRP3 inflammasome mediated IL-1beta production, ROS production and endosomal rupture. *Biomaterials* 31: 6833-6842.
19. Winter, M., H. D. Beer, V. Hornung, U. Krämer, R. P. Schins, and I. Förster. 2011. Activation of the inflammasome by amorphous silica and TiO2 nanoparticles in murine dendritic cells. *Nanotoxicology* 5: 326-340.
20. Yazdi, A. S., G. Guarda, N. Riteau, S. K. Drexler, A. Tardivel, I. Couillin, and J. Tschopp. 2010. Nanoparticles activate the NLR pyrin domain containing 3 (Nlrp3) inflammasome and cause pulmonary inflammation through release of IL-1α and IL-1β. *Proc. Natl. Acad. Sci. U. S. A.* 107: 19449-19454.
21. Jin, C. and R. A. Flavell. 2010. Molecular mechanism of NLRP3 inflammasome activation. *J. Clin. Immunol.* 30: 628-631.
22. Netea, M. G., C. A. Nold-Petry, M. F. Nold, L. A. Joosten, B. Opitz, J. H. van der Meer, F. L. van de Veerdonk, G. Ferwerda, B. Heinhuis, I. Devesa, C. J. Funk, R. J. Mason, B. J. Kullberg, A. Rubartelli, J. W. van der Meer, and C. A. Dinarello. 2009. Differential requirement for the activation of the inflammasome for processing and release of IL-1beta in monocytes and macrophages. *Blood* 113: 2324-2335.
23. Landmesser, U., S. Dikalov, S. R. Price, L. McCann, T. Fukai, S. M. Holland, W. E. Mitch, and D. G. Harrison. 2003. Oxidation of tetrahydrobiopterin leads to uncoupling of endothelial cell nitric oxide synthase in hypertension. *J. Clin. Invest.* 111: 1201-1209.
24. Sevier, C. S. and C. A. Kaiser. 2008. Ero1 and redox homeostasis in the endoplasmic reticulum. *Biochim. Biophys. Acta* 1783: 549-556.
25. Sorbara, M. T. and S. E. Girardin. 2011. Mitochondrial ROS fuel the inflammasome. *Cell Res.* 21: 558-560.
26. Shukla, R. K., A. Kumar, A. K. Pandey, S. S. Singh, and A. Dhawan. 2011. Titanium dioxide nanoparticles induce oxidative stress-mediated apoptosis in human keratinocyte cells. *J. Biomed. Nanotechnol.* 7: 100-101.
27. Ahmad, J., M. Ahamed, M. J. Akhtar, S. A. Alrokayan, M. A. Siddiqui, J. Musarrat, and A. A. Al-Khedhairy. 2012. Apoptosis induction by silica nanoparticles mediated through reactive oxygen species in human liver cell line HepG2. *Toxicol. Appl. Pharmacol.* 259: 160-168.
28. Bulua, A. C., A. Simon, R. Maddipati, M. Pelletier, H. Park, K. Y. Kim, M. N. Sack, D. L. Kastner, and R. W. Siegel. 2011. Mitochondrial reactive oxygen species promote production of proinflammatory cytokines and are elevated in TNFR1-associated periodic syndrome (TRAPS). *J. Exp. Med.* 208: 519-533.
29. Arnoult, D., F. Soares, I. Tattoli, and S. E. Girardin. 2011. Mitochondria in innate immunity. *EMBO Rep.* 12: 901-910.